# Dipole moments of the $\rho$ meson

M. B. Hecht and B. H. J. McKellar
*School of Physics, University of Melbourne, Parkville VIC 3052, Australia*
(Received 15 April 1997; revised manuscript received 26 November 1997)

The electric and magnetic dipole moments of the $\rho$ meson are calculated using the propagators and vertices derived from the QCD Dyson-Schwinger equations. Results obtained from using the Bethe-Salpeter amplitude studied by Chappell, Mitchell, and Tandy, and Pichowsky and Lee, are compared. The $\rho$ meson electric dipole moment is generated through the inclusion of a quark electric dipole moment, which is left as a free variable. These results are compared to the perturbative results to obtain a measure of the effects of quark interactions and confinement. The two dipole moments are also calculated using the phenomenological MIT bag model to provide a further basis for comparison. [S0556-2813(98)01405-8]

PACS number(s): 13.40.Em, 14.40.Cs, 11.10.St, 12.39.Ba

## I. INTRODUCTION

The electric and magnetic dipole moments of the $\rho$ meson, the lowest lying vector particle state, are calculated using the semiphenomenological $n$-point functions of quantum chromodynamics (QCD) obtained in the Dyson-Schwinger and Bethe-Salpeter framework. The $\rho$ meson is studied to provide some insight into the effect of QCD and confinement on the electromagnetic moments of hadrons, especially the question of the existence of a nonzero electric dipole moment (EDM) for the neutron and the applications this has to the study of $CP$ violation. In practice one is interested in these parameters for the nucleon and other hadrons, where they may be measured. But the study of the $\rho$ allows us to obtain insights without venturing into the complications of the three body system in QCD.

The Dyson-Schwinger equations are a series of coupled integral equations relating the $n$-point functions of QCD to one another. They provide a continuum method of calculation in the strong coupling regime of QCD and as such are able to relate the Greens functions of QCD to hadronic properties. For a review of this topic see [1]. The use of the Dyson-Schwinger and Bethe-Salpeter equations to calculate hadronic properties has been applied to pion observables [2–5], kaon electromagnetic form factors [6], $\rho$-$\omega$ mixing [7], and the anomalous $\gamma\pi^*\rightarrow\pi\pi$ form factor [8].

This calculation makes use of a model form for the quark propagator which ensures confinement by having no Lehmann representation, preventing free quark production thresholds, i.e., the quark cannot go ''on mass-shell.'' A phenomenological form for the $\rho$ amplitude, which models the momentum distribution of the quarks inside, and the finite size of, the $\rho$, is used, as well as the Ball-Chiu and Curtis-Pennington quark-photon vertex which ensures that both the Ward-Takahashi identity and multiplicative renormalizability are preserved. The $CP$-violating electric dipole term is introduced via a quark EDM which is left as a free parameter which can be varied.

Results obtained from using the Bethe-Salpeter amplitude studied by Mitchell and Tandy [7], Chappell [9], and Pichowsky and Lee [10], are compared. Perturbation theory results [11], which ignore the dressing of the vertex functions and propagators, are also included to observe the effect of using a quark propagator that correctly incorporates confinement and of modeling the dressed quark core of the $\rho$.

A phenomenological model, the MIT bag model, is also examined. This model incorporates relativistic, pointlike confined quarks but ignores one-gluon exchange and center of mass motion. Both the magnetic and electric dipole moments are calculated in the bag model providing a basis for comparison between the Dyson-Schwinger and Bethe-Salpeter framework and a purely phenomenological model, one that has been well studied over the years.

## II. THE DIPOLE MOMENTS

### A. The $\rho\rho\gamma$ vertex

The form for the $CP$-conserving $\rho\rho\gamma$ vertex is (see Fig. 1) [12],

$$d_\alpha^{\ \nu}(p)\Gamma_{\mu\nu\sigma}d_\beta^{\ \sigma}(p')=d_\alpha^{\ \nu}(p)\{(p+p')_\mu[-g_{\nu\sigma}\mathcal{E}(q^2)+q_\nu q_\sigma\mathcal{Q}(q^2)]+(g_{\mu\nu}q_\sigma-g_{\mu\sigma}q_\nu)\mathcal{M}(q^2)\}d_\beta^{\ \sigma}(p'), \quad (1)$$

where $d_{\alpha\beta}$ are the $\rho$ polarization vectors

$$d_{\alpha\beta}(k)=g_{\alpha\beta}-\frac{k_\alpha k_\beta}{k^2}. \quad (2)$$

The form factors $\mathcal{E}$, $\mathcal{Q}$, and $\mathcal{M}$ reduce in the limit as $q^2\rightarrow 0$ to $\mathcal{E}(0)=1$, $\mathcal{M}(0)=\mu$, the magnetic moment in units of $e/2m$, and $\mathcal{Q}(0)=(2/m^2)(Q+\mu-1)$, where $Q$ is the quadrupole moment in units of $e/m^2$.

### B. Projecting out charge and dipole terms

The integrals for the $\rho$ dipole moments that will be derived later, Eqs. (10) and (39), are too difficult to perform analytically. This means that to isolate relevant terms they will have to be projected out from the integral before it is calculated numerically. Defining

$$V_{\alpha\mu\beta}=d_\alpha^{\ \nu}(p)\Gamma_{\nu\mu\sigma}d_\beta^{\ \sigma}(p'), \quad (3)$$

and with the projection operator

 

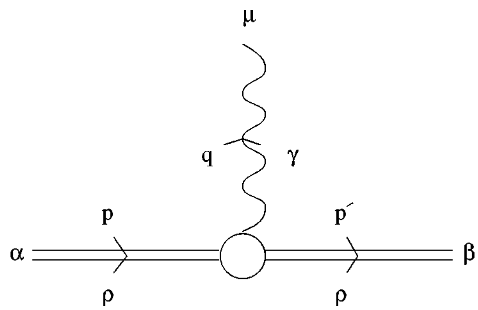


FIG. 1. The dressed $\rho\rho\gamma$ vertex.

$$P_1^{\alpha\mu\beta}=d^{\alpha}_{\ \nu'}(p)P^{\mu}(-g^{\nu'\sigma'})d^{\beta}_{\ \sigma'}(p'), \tag{4}$$

where $P_\mu=(p+p')_\mu$, the following result is obtained:

$$P_1^{\alpha\mu\beta}V_{\alpha\mu\beta}\xrightarrow{\lim q^2\to 0}12\mathcal{E}(0). \tag{5}$$

To project out the magnetic dipole term we use the following projection operator:

$$P_2^{\alpha\mu\beta}=d^{\alpha}_{\ \nu'}(p)\left[\frac{g^{\mu\nu'}q^{\sigma'}-g^{\mu\sigma'}q^{\nu'}}{q^2}+\frac{P^{\mu}g^{\nu'\sigma'}}{6p^2}\right]d^{\beta}_{\ \sigma'}(p'), \tag{6}$$

which is such that

$$P_2^{\alpha\mu\beta}V_{\alpha\mu\beta}\xrightarrow{\lim q^2\to 0}4\mathcal{M}(0). \tag{7}$$

### C. Quark contribution to the magnetic dipole moment

All calculations below, except those involving the bag model, are carried out in Euclidean space where $g_{\mu\nu}=\delta_{\mu\nu}$, $\gamma_\mu=\gamma_\mu^\dagger$ and $\{\gamma_\mu,\gamma_\nu\}=2\delta_{\mu\nu}$.

The impulse approximation to the quark contribution to the magnetic dipole moment is given by (see Fig. 2)

$$M_{fi}=\sum_{\text{flavor}=u,d}\varepsilon^{\alpha}(p)\varepsilon^{\mu}(q)\varepsilon^{\beta}(p')eQ_{\text{flavor}}I^{\text{flavor}}_{\alpha\mu\beta}. \tag{8}$$

$Q_{\text{flavor}}$ is the charge of the quark interacting with the photon. The $u$ and $d$ quarks are treated as identical except for their charge and so the contribution becomes

$$M_{fi}=\varepsilon^{\alpha}(p)\varepsilon^{\mu}(q)\varepsilon^{\beta}(p')eI_{\alpha\mu\beta}, \tag{9}$$

$$\begin{aligned}I_{\alpha\mu\beta}=(-1)\int\frac{d^4k}{(2\pi)^4}\,&\mathrm{tr}_{CFD}[\Gamma^{\rho}_{\beta}(k;p-q)\\&\times S(k_{-+})\imath\Gamma^{\mathrm{BC+CP}}_{\mu}(k_{++},k_{-+})\\&\times S(k_{++})\Gamma^{\rho}_{\alpha}(k+q/2;p)S(k_{+-})].\end{aligned} \tag{10}$$

Where $k_{\alpha\beta}=k+(\alpha q/2)+(\beta p/2)$, $\Gamma^{\rho}$ refers to the $\rho$ meson amplitude, $\Gamma^{\mathrm{BC+CP}}_{\mu}$ is the dressed quark-photon vertex, and $S(p)$ is the dressed quark propagator for a quark of momentum $p$, which will all be discussed in detail below.

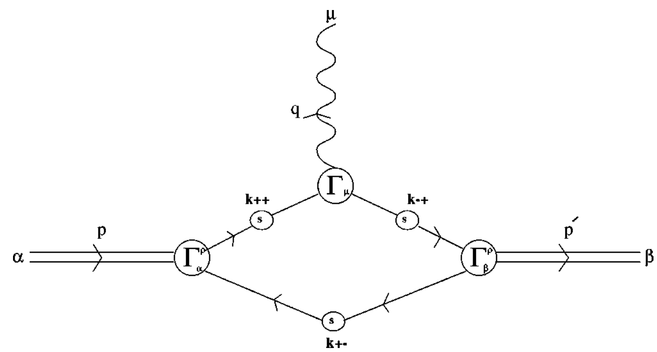


FIG. 2. The quark contribution to the dipole moments of the $\rho$, with $S$ the dressed quark propagators, $\Gamma_\mu$ the dressed quark-photon vertex, and $\Gamma^{\rho}$ the $\rho$-quark vertex.

### D. Quark propagators

The general form for the solution to the quark propagator Dyson-Schwinger equation [1] is

$$\begin{aligned}S(p)&=-\imath\not{p}\sigma_V(p^2)+\sigma_S(p^2)\\&=[\imath\not{p}A(p^2)+B(p^2)]^{-1}.\end{aligned} \tag{11}$$

A model form for the propagator is given by [3,4]

$$\begin{aligned}\bar{\sigma}_S(x)=&\,C_{\bar{m}}e^{-2x}+\left(\frac{1-e^{-b_1x}}{b_1x}\right)\left(\frac{1-e^{-b_3x}}{b_3x}\right)\\&\times\left[b_0+b_2\left(\frac{1-e^{-\Lambda x}}{\Lambda x}\right)\right]\\&+\frac{\bar{m}}{x+\bar{m}^2}(1-e^{-2(x+\bar{m}^2)}),\end{aligned} \tag{12}$$

$$\bar{\sigma}_V(x)=\frac{2(x+\bar{m}^2)-1+e^{-2(x+\bar{m}^2)}}{2(x+\bar{m}^2)^2}-\bar{m}C_{\bar{m}}e^{-2x}, \tag{13}$$

where $x=p^2/2D$, $\bar{\sigma}_V(x)=(2D)\sigma_V(p^2)$, $\bar{\sigma}_S=\sqrt{2D}\sigma_S(p^2)$, and $\bar{m}=m/\sqrt{2D}$, $D$ is a mass scale. [$\Lambda=10^{-4}$ is chosen to decouple the small and large spacelike-$p^2$ behavior in Eq. (12); i.e., to allow for $b_0$ to govern the ultraviolet behavior and $b_2$ the infrared.] The parameters $C_{\bar{m}}$, $\bar{m}$, $b_0,\dots,b_3$ are [6]

$$\begin{aligned}C_{\bar{m}\neq 0}&=0.0,\\C_{\bar{m}=0}&=0.121,\\\bar{m}&=0.00897,\\b_0&=0.131,\\b_1&=2.90,\\b_2&=0.603,\\b_3&=0.185,\end{aligned} \tag{14}$$

with the mass scale $D=0.160\ \mathrm{GeV}^2$ chosen to give the correct value for $f_\pi$. This form for the quark propagator is based upon studies of the Dyson-Schwinger equation for $S(p)$ using a gluon propagator with an infrared singularity,

$$g^2 D_{\mu\nu}(k) \equiv \left( \delta_{\mu\nu} - \frac{k_\mu k_\nu}{k^2} \right) 8\pi^4 D \delta^4(k), \tag{15}$$

and a dressed quark-gluon vertex [4,6]. Quark confinement is characterized by the nonobservation of free quark states. A pole in the quark propagator in the timelike region would be a sign of a free quark state, just as a free bound state is manifest as a pole in a $n$-point Greens function. Thus a sufficient condition for the lack of free quark production thresholds is the absence of timelike poles in the propagator. The model quark propagator given above is an entire function (except at timelike $p^2 = \infty$) and so does not have a Lehmann representation. This means it can be interpreted as describing a confined particle and it ensures the lack of the unphysical singularities corresponding to free quarks in $I_{\alpha\mu\beta}$.

The dipole moments are also calculated using a form for the quark propagator developed by Mitchell and Tandy [7], to investigate $\rho$-$\omega$ mixing. This propagator is given by

$$\bar{\sigma}_S(x) = C_{\bar{m}} e^{-2x} + \frac{\bar{m}}{x}(1 - e^{-2x}), \tag{16}$$

$$\bar{\sigma}_V(x) = \frac{e^{-2x} - (1-2x)}{2x^2} - \bar{m} C_{\bar{m}} e^{-2x}. \tag{17}$$

To fix the parameters $\lambda = \sqrt{2D}$ and $C_{\bar{m}}$, a fit to $\langle \bar{q}q \rangle$, $f_\pi$, $r_\pi$ and the $\pi$-$\pi$ scattering lengths was done. With $\frac{1}{2}(m_u + m_d) = 16$ MeV a best fit was obtained for $\lambda = 0.889$ GeV and $C_{\bar{m}} = 0.581$ [7]. This form has a deficiency which can be seen in its failure to correctly model the behavior of $\sigma_S$ away from $x = 0$, in the massless limit with dynamically broken chiral symmetry [4]. The large value for the mass of the quark used is related to the deficiency of the propagator mentioned above [13].

### E. ρ-meson amplitude

The dominant Bethe-Salpeter amplitude for the $\rho$ meson is given by [14,15],

$$\Gamma^l_{\rho\ \mu}(k,p) = \imath \left( \gamma_\mu - \frac{\not{p} p_\mu}{p^2} \right) \tau^l \frac{\Gamma_\rho(k,p)}{N_\rho}, \tag{18}$$

where $k$ is the relative momentum of the quark and antiquark, $p$ is the momentum of the $\rho$ meson, and $l$ and $\mu$ are flavor and Dirac indices, respectively. This form ignores other allowable Dirac structure in the vector meson Bethe-Salpeter amplitude and so introduces errors of the order of 10% [5]. Using the quark propagator defined in Eqs. (12) and (13) and a Ball-Chiu quark-photon vertex (see later), Chappell uses the following approximate form for $\Gamma_\rho(k,p)$ [9]:

$$\Gamma_\rho = e^{-k^2/a_1^2} + \frac{a_2}{1 + (k^2/\alpha a_1)}, \tag{19}$$

with $a_1 = 0.38845$, $a_2 = 0.01478$, $\alpha = 2$. The values for the parameters were found by fitting to the experimental values of $f_\rho$ and $g_{\rho\pi\pi}$ [9]. Pichowsky and Lee, also using the quark propagator defined in Eqs. (12) and (13) and a quark-photon vertex of the Ball-Chiu type, use an identical form for $\Gamma_\rho$, given by [10]

$$\Gamma_\rho(k,p) = e^{-k^2/a_V^2} + \frac{c_V}{1 + k^2/b_V^2}. \tag{20}$$

Fitting to the experimental values for $f_\rho$ and $g_{\rho\pi\pi}$ they obtain values for the parameters of $a_V = 0.400$, $b_V = 0.008$, and $c_V = 125.0$. Using the quark propagator defined in Eqs. (16) and (17) Mitchell and Tandy use a form for the amplitude $\Gamma_\rho$ given by

$$\Gamma_\rho(k,p) = e^{-k^2/a^2}, \tag{21}$$

where $a = 0.194$ GeV. The normalization for the $\rho$ amplitude is fixed by [10]

$$p_\mu \left( \delta_{\alpha\beta} - \frac{p_\alpha p_\beta}{p^2} \right) = N_c \operatorname{tr}_D \int \frac{d^4k}{(2\pi)^4} \frac{\partial S(k_+)}{\partial p_\mu} \times \Gamma_{\rho\alpha}(k,p) S(k_-) \Gamma_{\rho\beta}(k,p) + N_c \operatorname{tr}_D \int \frac{d^4k}{(2\pi)^4} S(k_+) \times \Gamma_{\rho\alpha}(k,p) \frac{\partial S(k_-)}{\partial p_\mu} \Gamma_{\rho\beta}(k,p), \tag{22}$$

where $k_\alpha = k + (\alpha p/2)$. This condition, along with the fact that the quark-photon vertex given below obeys the Ward Identity, ensures that $\mathcal{E}(q^2 = 0) = 1$, i.e., that the $\rho$ has unit charge [4].

Using the transformation properties $S^T(-k) = C^\dagger S(k) C$, $\Gamma^{\rho T}_\alpha(-k,p) = -C^\dagger \Gamma^\rho_\alpha(k,p) C$, and $\Gamma^{\mathrm{BC+CP}\ T}_\mu(-p,-q) = -C^\dagger \Gamma^{\mathrm{BC+CP}}_\mu(p,q) C$, where $C = \gamma_2 \gamma_4$ is the charge conjugation operator, and the Ward-Takahashi Identity, one can show that current conservation holds [4], i.e.,

$$q_\mu I_{\alpha\mu\beta} = 0. \tag{23}$$

Given a description for the quark-photon vertex, the dipole moments of the $\rho$ can now be calculated using Eqs. (12), (13), and (19); (12), (13), and (20); and (16), (17), and (21).

### F. Quark-photon vertex

The quark-photon vertex also satisfies its own Dyson-Schwinger equation, but solving this integral equation is difficult. Despite this, a realistic ansatz for the vertex function has been developed by constraining its form using certain criteria [16–18]. The quark-photon vertex ansatz thus obtained is given by

$$\Gamma^{\mathrm{BC+CP}}_\mu(p,q) = \Gamma^{\mathrm{BC}}_\mu(p,q) + \Gamma^{\mathrm{CP}}_\mu(p,q). \tag{24}$$

The Ball-Chiu vertex $\Gamma^{\mathrm{BC}}_\mu$ has the form [18]

$$\Gamma_{\mu}^{\rm BC}(p,q)=\frac{A(p^2)+A(q^2)}{2}\gamma_\mu+\frac{(p+q)_\mu}{p^2-q^2}\left[\frac{1}{2}[A(p^2)-A(q^2)](\not p+\not q)-\imath[B(p^2)-B(q^2)]\right]. \quad (25)$$

This vertex ansatz is completely described by the dressed quark propagator and satisfies both the Ward-Takahashi and Ward identities, is free of kinematic singularities as $q^2\to p^2$, transforms correctly under appropriate transformations, and reduces to the perturbative limit. To ensure multiplicative renormalizability Curtis and Pennington added a transverse piece to the Ball-Chiu vertex [19]. This term has the form given below:

$$\Gamma_{\mu}^{\rm CP}(p,q)=\left(\frac{-\imath\gamma_\mu(p^2-q^2)-(p+q)_\mu(\not p-\not q)}{2d(p,q)}\right)\times[A(p^2)-A(q^2)], \quad (26)$$

with

$$d(p,q)=\frac{1}{p^2+q^2}\{(p^2-q^2)^2+[M^2(p^2)+M^2(q^2)]^2\}, \quad (27)$$

$$M(p^2)=\frac{B(p^2)}{A(p^2)}.$$

### G. The magnetic dipole moment

The dipole moment can now be calculated. The color, flavor, and Dirac traces are performed for the integral $I_{\alpha\mu\beta}$, given in Appendix A, and the charge and dipole terms projected out using the projection operators outlined above. The integrals are performed and the dipole calculated using

$$\mu=\lim_{q^2\to 0}\mathcal{M}(q^2)=\lim_{q^2\to 0}P_2^{\alpha\mu\beta}I_{\alpha\mu\beta}/4. \quad (28)$$

The calculation is performed in the Breit frame where

$$q=(0,0,Q,0),$$

$$p=(0,0,Q/2,\imath\sqrt{m_\rho^2+Q^2/4}),$$

$$p'=(0,0,-Q/2,\imath\sqrt{m_\rho^2+Q^2/4}).$$

A transformation to four-dimensional hyperspherical coordinates is carried out so that

$$k=|k|(\sin\beta\sin\theta\cos\phi,\sin\beta\sin\theta\sin\phi,\sin\beta\cos\theta,\cos\beta), \quad (29)$$

with

TABLE I. Magnetic dipole moment $\mu$ in units of $e/2m$.

| $\rho$ amplitude/quark propagator | $\mu$ |
|---|---|
| Chappell [9] | 3.01 |
| Pichowsky and Lee [10] | 2.72 |
| Mitchell and Tandy [7] | 2.57 |
| Perturbative result [11] | 2.00 |
| Nonrelativistic SU(6) [20], constituent quark mass from [23] | 2.26 |

$$\int d^4k=\int_0^\infty k^3dk\int_0^\pi\sin^2\beta d\beta\int_0^\pi\sin\theta d\theta\int_0^{2\pi}d\phi. \quad (30)$$

There is no $\phi$ dependence in the integrand so the $\phi$ integral is performed analytically, contributing a factor of $2\pi$.

The integral is then performed numerically using Gaussian quadrature methods to obtain the results given in Table I. The results obtained using the framework of Chappell, and Pichowsky and Lee, are within 10% of each other which is indicative of the similarities of the approaches. The perturbative result from [11], and the nonrelativistic SU(6) result are given for comparison. The later result is simply [20]

$$\mu_{\rho^+}=\frac{e}{2m_q}. \quad (31)$$

In Eq. (31) the quark mass is to be interpreted a constituent quark mass of, say, 340 MeV [21], which gives $\mu_{\rho^+}=2.26\ e/2m_\rho$. Thus one could say that the effect of QCD as interpreted in our calculation is to convert $m_q$ from the current quark value to an appropriate constituent quark value. Note that the improper use of a current quark mass in Eq. (31) gives the large value $\mu_{\rho^+}=152\ e/2m_\rho$.

### H. The electric dipole moment

$CP$ violation is a feature of the weak interaction which is not well understood at present. It will, in principle, give rise to electric dipole moments for quarks and hadrons. In calculating hadronic electric dipole moments, the question of the effects of confinement and QCD in going from the quark EDM to the hadron EDM have not been studied. Here we study these effects for the $\rho$ meson.

The magnetic dipole of the $\rho$ meson comes from the term in the Salam-Delbourgo vertex function

$$(g_{\alpha\mu}q_\beta-g_{\beta\mu}q_\alpha)\mathcal{M}.$$

This results in a term in the $\rho\rho\gamma$ matrix element that looks similar to

$$\varepsilon(p)\cdot F\cdot\varepsilon(p')\mathcal{M},$$

where

$$F_{\alpha\beta}=\partial_\beta A_\alpha-\partial_\alpha A_\beta$$

is the electromagnetic field tensor. To find the vertex function term that contributes to the electric dipole moment the familiar correspondence is used:

$$F_{\alpha\beta} \to \tilde{F}_{\alpha\beta} = \frac{1}{2}\varepsilon_{\alpha\beta\mu\nu}F^{\mu\nu}$$

$$\mathcal{M}(q^2) \to \mathcal{D}(q^2), \tag{32}$$

where $\mathcal{D}(0)=d$, the electric dipole moment in units of $e/2m$. Thus as

$$\frac{1}{2}\varepsilon_{\alpha\beta\mu\nu}F^{\mu\nu} = \varepsilon_{\alpha\beta\mu\nu}A^{\mu}q^{\nu},$$

the term in the $\rho\rho\gamma$ vertex that defines the $\rho$ EDM is

$$\varepsilon_{\alpha\beta\mu\nu}q^{\nu}\mathcal{D}(q^2). \tag{33}$$

Once again the electric and dipole terms will need to be projected out. The vertex function is given by

$$V^{\mathrm{EDM}}_{\alpha\mu\beta} = d_{\alpha}^{\ \nu}(p)\Gamma_{\nu\mu\sigma}d_{\sigma}^{\ \beta}(p') = d_{\alpha}^{\ \nu}(p)\{P_{\mu}(-g_{\nu\sigma}\mathcal{E}(q^2) + q_{\nu}q_{\sigma}\mathcal{Q}(q^2)] + (g_{\mu\nu}q_{\sigma} - g_{\mu\sigma}q_{\nu})\mathcal{M}(q^2) + \varepsilon_{\nu\sigma\mu\rho}q^{\rho}\mathcal{D}(q^2)\}d_{\beta}^{\ \sigma}(p'). \tag{34}$$

Using a projection operator of the form

$$P_3^{\alpha\mu\beta} = -\left(\frac{1}{2q^2}\right)d^{\alpha\nu'}(p)\varepsilon_{\nu'\ \sigma'}^{\ \mu\rho}q_{\rho}d^{\beta\sigma'}(p'), \tag{35}$$

the result

$$P_3^{\alpha\mu\beta}V_{\alpha\mu\beta} \xrightarrow{\lim q\to 0} \mathcal{D}(0) \tag{36}$$

follows.

### I. Quark contribution to the electric dipole moment

To introduce an electric dipole moment in the impulse approximation the $qq\gamma$ vertex needs to be modified to introduce a $CP$-violating term. Thus the following vertex is used:

$$\Gamma_{\mu}(p,q) = \Gamma_{\mu}^{\mathrm{BC+CP}}(p,q) - \imath D_q\gamma_5\sigma_{\mu\rho}(p-q)^{\rho}, \tag{37}$$

where $D_q$ is the EDM of the quark. This form for the $qq\gamma$ vertex still ensures that both the Ward-Takahashi and Ward identities are preserved, is free of kinematic singularities as $q^2 \to p^2$ and reduces to the perturbative limit. It also still preserves multiplicative renormalizability. However we have ignored any structure of the $CP$-violating term which may be generated by strong or electromagnetic interactions.

Following the same procedure as outlined above, the impulse approximation to the EDM is given by

$$\mathcal{M}_{fi} = \varepsilon^{\alpha}(p)\varepsilon^{\mu}(q)\varepsilon^{\beta}(p')eI^{\mathrm{EDM}}_{\alpha\mu\beta}, \tag{38}$$

where the integral $I^{\mathrm{EDM}}_{\alpha\mu\beta}$ is given by

$$I^{\mathrm{EDM}}_{\alpha\mu\beta} = (-1)\int\frac{d^4k}{(2\pi)^4}\ \mathrm{tr}_{CFD}[\Gamma_{\beta}^{\rho}(k;p-q) S(k_{-+})\imath\Gamma_{\mu}(k_{++},k_{-+}) \times S(k_{++})\Gamma_{\alpha}^{\rho}(k+q/2;p)S(k_{+-})]. \tag{39}$$

TABLE II. Electric dipole moment $d_\rho$ in units of $d_q$ $e$ cm.

| $\rho$ amplitude/quark propagator | $d_\rho$ |
|---|---|
| Chappell [9] | 0.743 |
| Pichowsky and Lee [10] | 0.779 |
| Mitchell and Tandy [7] | 0.627 |
| Perturbative result [11], $m_q$ from [9,10] | 0.010 |

The expanded form of the integral $I^{\mathrm{EDM}}_{\alpha\mu\beta}$ is given in Appendix B. The EDM can now be calculated. Once again the Dirac traces are performed and the charge and electric dipole terms projected out using the projection operators given above. The integrals are performed and the dipole calculated using

$$d = \lim_{q^2\to 0}\mathcal{D}(q^2) = \lim_{q^2\to 0}P_3^{\alpha\mu\beta}I^{\mathrm{EDM}}_{\alpha\mu\beta}. \tag{40}$$

The integral is again evaluated in the Breit frame.

The dipole interaction between the quark and the photon is governed by the term

$$D_u\bar{u}\gamma_5\sigma^{\mu\nu}q_{\nu}uA_{\mu} + D_d\bar{d}\gamma_5\sigma^{\mu\nu}q_{\nu}dA_{\mu}, \tag{41}$$

where the $D_u$ and $D_d$ are the electric dipole moments for the $u$ and $d$ quarks, respectively. In many models $D \propto Q$ for quarks, so the following form is used:

$$D_{\{u,d\}} = Q_{\{u,d\}}d_q. \tag{42}$$

The perturbative result has been calculated and it gives

$$d^{\mathrm{pert}} = 3m_qd_q \tag{43}$$

in units of $e/2m$. The quark electric dipole moment has been left as a free parameter and so an estimate of the size of $d_q$ is needed. The quark electric dipole moment can be generated in various models. One of these is the Weinberg model of three Higgs doublets [22]. In this model the quark EDM comes about due to neutral Higgs exchange with the quark dipole moment given by [23]

$$d_q = \frac{eG_F}{\sqrt{2}\pi^2}m_q\sum_i X_i'Y_i'\frac{m_q^2}{m_{Hi}^2}\ln\frac{m_q^2}{m_{Hi}^2}, \tag{44}$$

where the $m_{Hi}$ are the masses of the neutral Higgs and $X_i'$ and $Y_i'$ are mixings of the neutral Higgs. This gives a quark dipole moment of the order of $10^{-24}$ $e$ cm. Thus we obtain the results for the $\rho$ electric dipole moment, in units of $d_q$, listed in Table II. Again the perturbative result is included for comparison. For completeness, it is noted that the nonrelativistic result is given by $d_\rho = d_q$ $e$ cm. The results from the Chappell, and Pichowsky and Lee amplitudes are again seen to be very close, as was the case for the magnetic moment.

## III. THE BAG MODEL

There are purely phenomenological models that have been used over the years to describe the properties of hadrons. One successful and popular model which incorporates many of the features of QCD is the MIT bag model [24,25]. The MIT bag model includes relativistic, pointlike, confined quarks and provides a phenomenological description of the nonperturbative gluon interactions. The simplest form of the MIT model will be used, with one-gluon exchange and center of mass motion ignored. While these results, at least for the magnetic moments of baryons, are well known we discuss them here to provide another point of comparison for the results of Sec. II.

The starting point for the bag model is the assumption of free quarks confined within a spherical volume of radius $R$. Solving the Dirac equation inside the sphere results in a wave function given by [25,26]

$$\psi(r)=\frac{N(x)}{\sqrt{4\pi}}\begin{pmatrix}\sqrt{\frac{w+m}{w}}j_0\left(\frac{xr}{R}\right)\chi\\ \sqrt{\frac{w-m}{w}}\imath\boldsymbol{\sigma}\cdot\hat{\mathbf{r}}j_1\left(\frac{xr}{R}\right)\chi\end{pmatrix}, \tag{45}$$

where $w(m,R)=\sqrt{m_q^2+x^2/R^2}$, $j_0$ and $j_1$ are spherical Bessel functions and $x$ is the quark momentum in units of $1/R$. The normalization $N(x)$ is given by

$$N^{-2}(x)=R^3j_0^2(x)\frac{2w(w-1/R)+m_q/R}{w(w-m)}, \tag{46}$$

and the eigenfrequency $x$ by

$$\tan x=\frac{x}{1-m_qR-[x^2+(m_qR)^2]^{1/2}}, \tag{47}$$

arising from the boundary condition

$$-\imath\boldsymbol{\gamma}\cdot\hat{\mathbf{r}}\psi=\psi \tag{48}$$

at $r=R$. To confine the quarks a ''pressure'' $B$ is introduced which ensures energy-momentum conservation and confinement. Thus the total energy of the bag becomes

$$E(R)=\sum_i N_i(m_{qi}^2+x^2/R^2)^{1/2}+B\frac{4}{3}\pi R^3, \tag{49}$$

where $N_i$ is the number of quarks or type $i$ inside the bag. The stability of the bag also implies that

$$\frac{\partial E(R)}{\partial R}=0. \tag{50}$$

All calculations will be carried out in the rest frame of the bag and so $E(R)$ will be equated with $m_\rho$. Equations (47), (49), and (50) will then be used to fix the variables $x$, $R$, and $B$.

TABLE III. Magnetic dipole moment $\mu$ in the bag model in units of $e/2m$.

| Mass of quark | $\mu$ |
|---|---|
| $m_q$ from [9,10] | 2.21 |
| Chappell [9] | 3.01 |
| Pichowsky and Lee [10] | 2.72 |
| Mitchell and Tandy [7] | 2.57 |

### A. Magnetic moment in the bag model

The magnetic moment is given by

$$\boldsymbol{\mu}=\frac{1}{2}\int d^3\mathbf{r}\,\mathbf{r}\times\mathbf{j}_{em} \tag{51}$$

$$=\frac{1}{2}\int d^3\mathbf{r}\,\mathbf{r}\times\sum_i(\overline{\psi_i}\boldsymbol{\gamma}\psi_i)Q_ie,$$

where the summation is over the quarks. This gives [26,21]

$$\boldsymbol{\mu}_{\boldsymbol{\rho}}=\mu_q\sum_i\boldsymbol{\sigma}_iQ_i, \tag{52}$$

where $\mu_q$, the magnetic dipole moment of the quark, is given by

$$\mu_q=\frac{e}{2m_q}\frac{1}{3}m_qR\frac{4wR+2m_qR-3}{2(wR)^2-2wR+m_qR}. \tag{53}$$

Using the standard spin-flavor wave function of the $\rho$ yields the results, listed in Table III, and discussed in the final section of this paper.

### B. Electric dipole moment in the bag model

Using the single particle wave function from above, and the $P$ and $CP$ violating electromagnetic current

$$J_{\mu\nu}=-\imath D_q\overline{\psi}\gamma_5\sigma_{\mu\nu}\psi, \tag{54}$$

where $\sigma_{\mu\nu}=\imath/2[\gamma_\mu,\gamma_\nu]$, it can be shown that

$$J_{\mu\nu}F^{\mu\nu}=-D_q\overline{\psi}\boldsymbol{\sigma}\psi\cdot\mathbf{E}+\text{terms involving }\mathbf{B}, \tag{55}$$

where $F^{\mu\nu}$ is the standard electromagnetic tensor. Therefore [27]

$$\mathbf{d}_\rho=\int_{\text{bag}}\left\langle\rho\uparrow\left|\sum_{\text{quarks}}D_q\overline{\psi}\boldsymbol{\sigma}\psi\right|\rho\uparrow\right\rangle$$

$$=N^2\int_0^R dr\,r^2\left[j_0^2\left(\frac{xr}{R}\right)+\frac{1}{3}j_1^2\left(\frac{xr}{R}\right)\right]$$

$$\times\left\langle\rho\uparrow\left|\sum_{\text{quarks}}D_q\boldsymbol{\sigma}\right|\rho\uparrow\right\rangle. \tag{56}$$

Thus, again using the $\rho$ spin-flavor wave function, the following formula for the EDM of the $\rho$ is obtained:

TABLE IV. Electric dipole moment in the bag model in units of $d_q$ $e$ cm.

| Mass of quark | $d_\rho$ |
|---|---|
| $m_q$ from [9,10] | 0.828 |
| Chappell [9] | 0.743 |
| Pichowsky and Lee [10] | 0.779 |
| Mitchell and Tandy [7] | 0.627 |

$$d_\rho = N^2 \int_0^R dr\, r^2 \left[ j_0^2\left(\frac{xr}{R}\right) + \frac{1}{3} j_1^2\left(\frac{xr}{R}\right) \right] \quad (57)$$

in units of $d_q$ $e$ cm. This leads to the results given in Table IV and discussed below.

## IV. DISCUSSION

Using a model form for the quark propagator obtained from the Dyson-Schwinger equations, two different phenomenological $\rho$-meson amplitudes fitted to $f_\rho$ and $g_{\rho\pi\pi}$ and one used to describe $\rho$-$\omega$ mixing, and a dressed quark-photon vertex, the $\rho$ dipole moments have been calculated.

All three nonperturbative models used agree qualitatively with the amplitude and propagator defined in [9] yielding the largest value for $\mu_\rho$ and that of [7] the smallest. The Bethe-Salpeter amplitude of [10] resulted in the largest value for $d_\rho$, with that of [7] yielding the smallest. Thus the values calculated for the $\rho$ magnetic and electric dipole moments are fairly robust when it comes to slight changes in the forms for both the quark propagator and the $\rho$ Bethe-Salpeter amplitude.

As seen above the inclusion of quark confinement gives greatly enhanced values over those obtained using perturbation theory. The nonperturbative results for the magnetic dipole moment are ~29–51 % bigger than the perturbative result. While the electric dipole moment showed an even greater increase, being ~63–78 times larger than the value obtained with perturbation theory. $d_\rho$ is linearly dependent upon the quark dipole moment and so a different model for the quark moment could change the value for $d_\rho$ substantially. Conversely, an experimental measure for $d_\rho$ would put a limit on $d_q$ and possibly rule out some models.

The increase in the dipole moments is due to the inclusion of quark propagators that ensure confinement and a more accurate modeling of the momentum distribution and finite size of the $\rho$ meson. The kernel of the Bethe-Salpeter equation involves the dressed quark and gluon propagators and so includes the effects of the quark-gluon sea. The amplitudes that have been used here can thus be said to model these effects phenomenologically.

These calculations extend the process of using the Dyson-Schwinger and Bethe-Salpeter framework to obtain hadron properties to the $\rho$ meson.

The $\rho$ dipole moments have also been calculated in the MIT bag model. This phenomenological model also includes confinement via the introduction of the ‘‘pressure’’ term $B$. The bag is also assumed to incorporate the effects of the nonperturbative gluon exchange and interaction. This relativistic, confining model also yields values for the dipole moments greater than that of perturbation theory, as was the case for the results using the DSE and BSE framework, i.e., the results from both approaches agree qualitatively. The magnetic dipole moment is about ~10% bigger than the perturbative result, smaller than any of the results obtained in the impulse approximation. The electric dipole calculation was ~6% bigger than the largest result using the Dyson-Schwinger and Bethe-Salpeter equations and ~83 times bigger than the perturbative result. Again the inclusion of confinement has led to an enhancement in the dipole moments of the $\rho$. Indeed, one could suggest that for the calculation of the magnetic and electric dipole moments, the bag model gives a reasonable estimate of the effects of confinement.

The $\rho$ meson has been used in this study, not because there is any realistic possibility of measuring the electromagnetic moments we have calculated, but to provide some insight into the effects of QCD and confinement on calculations of these moments in the hope of obtaining insight into the effects these aspects of quark dynamics may have on estimates of the electromagnetic moments of hadrons [28,29].

## ACKNOWLEDGMENTS

M.B.H. wishes to thank C. D. Roberts for helpful discussions and for pointing out the work of I. Chappell. This work was supported in part by the Australian Research Grants Committee, and the Australian Department of Industry, Science and Tourism.

## APPENDIX A: INTEGRAL FOR THE MAGNETIC DIPOLE MOMENT

With the definitions given above the integral $I_{\alpha\mu\beta}$ becomes (after color and flavor traces)

$$\begin{aligned} I_{\alpha\mu\beta} = \frac{2\imath N_c}{N_\rho^2} \int \frac{d^4k}{(2\pi)^4} \Gamma_\rho(k)\Gamma_\rho(k+q/2)\ \mathrm{tr}_D[ & \gamma_\beta \not{k}_{-+} \gamma_\mu \not{k}_{++} \gamma_\alpha \not{k}_{+-} T_1 + \gamma_\beta \not{k}_{-+} \gamma_\mu \gamma_\alpha T_2 + \gamma_\beta \not{k}_{-+} \gamma_\alpha \not{k}_{+-} k_{0+\mu} T_3 \\ & + \gamma_\beta \not{k}_{-+} \not{k}_{++} \gamma_\alpha k_{0+\mu} T_4 + \gamma_\beta \not{k}_{++} \gamma_\alpha \not{k}_{+-} k_{0+\mu} T_5 + \gamma_\beta \gamma_\alpha k_{0+\mu} T_6 + \gamma_\beta \not{k}_{-+} \gamma_\alpha \not{k}_{+-} k_{0+\mu} T_7 \\ & + \gamma_\beta \not{k}_{-+} \not{k}_{++} \gamma_\alpha k_{0+\mu} T_8 + \gamma_\beta \gamma_\mu \gamma_\alpha \not{k}_{+-} T_9 + \gamma_\beta \gamma_\mu \not{k}_{++} \gamma_\alpha T_{10} + \gamma_\beta \not{k}_{++} \gamma_\alpha \not{k}_{+-} k_{0+\mu} T_{11} + \gamma_\beta \gamma_\alpha k_{0+\mu} T_{12} \\ & + \gamma_\beta \not{k}_{-+} \gamma_\alpha \not{k}_{+-} k_{0+\mu} T_{13} + \gamma_\beta \not{k}_{-+} \not{k}_{++} \gamma_\alpha k_{0+\mu} T_{14} + \gamma_\beta \not{k}_{++} \gamma_\alpha \not{k}_{+-} k_{0+\mu} T_{15} + \gamma_\beta \gamma_\alpha k_{0+\mu} T_{16}], \end{aligned} \quad \text{(A1)}$$

where the terms with an odd number of $\gamma$ matrices have been dropped. The $T_{1-16}$ are defined as follows:

$$T_1 = \imath(V_1 + V_4)\sigma_V(k_{-+}^2)\sigma_V(k_{++}^2)\sigma_V(k_{+-}^2),$$

$$T_2=-\imath(V_1+V_4)\sigma_V(k_{-+}^2)\sigma_S(k_{++}^2)\sigma_S(k_{+-}^2),$$

$$T_3=2\imath k_{++}^2(V_2+V_5)\sigma_V(k_{-+}^2)\sigma_V(k_{++}^2)\sigma_V(k_{+-}^2),$$

$$T_4=-2\imath(V_2+V_5)\sigma_V(k_{-+}^2)\sigma_S(k_{++}^2)\sigma_S(k_{+-}^2),$$

$$T_5=2\imath k_{-+}^2(V_2-V_5)\sigma_V(k_{-+}^2)\sigma_V(k_{++}^2)\sigma_V(k_{+-}^2),$$

$$T_6=-2\imath k_{-+}^2(V_2-V_5)\sigma_V(k_{-+}^2)\sigma_S(k_{++}^2)\sigma_S(k_{+-}^2),$$

$$T_7=-2V_3\sigma_V(k_{-+}^2)\sigma_S(k_{++}^2)\sigma_V(k_{+-}^2),$$

$$T_8=-2V_3\sigma_V(k_{-+}^2)\sigma_V(k_{++}^2)\sigma_S(k_{+-}^2),$$

$$T_9=-\imath(V_1+V_4)\sigma_S(k_{-+}^2)\sigma_S(k_{++}^2)\sigma_V(k_{+-}^2),$$

$$T_{10}=-\imath(V_1+V_4)\sigma_S(k_{-+}^2)\sigma_V(k_{++}^2)\sigma_S(k_{+-}^2),$$

$$T_{11}=-2\imath(V_2+V_5)\sigma_S(k_{-+}^2)\sigma_S(k_{++}^2)\sigma_V(k_{+-}^2),$$

$$T_{12}=-2\imath k_{++}^2(V_2+V_5)\sigma_S(k_{-+}^2)\sigma_V(k_{++}^2)\sigma_S(k_{+-}^2),$$

$$T_{13}=-2\imath(V_2-V_5)\sigma_S(k_{-+}^2)\sigma_S(k_{++}^2)\sigma_V(k_{+-}^2),$$

$$T_{14}=-2\imath(V_2-V_5)\sigma_S(k_{-+}^2)\sigma_V(k_{++}^2)\sigma_S(k_{+-}^2),$$

$$T_{15}=-2V_3\sigma_S(k_{-+}^2)\sigma_V(k_{++}^2)\sigma_V(k_{+-}^2),$$

$$T_{16}=2V_3\sigma_S(k_{-+}^2)\sigma_S(k_{++}^2)\sigma_S(k_{+-}^2), \tag{A2}$$

with

$$V_1=\frac{A(k_{++}^2)+A(k_{-+}^2)}{2},$$

$$V_2=\frac{A(k_{++}^2)-A(k_{-+}^2)}{2(k_{++}^2-k_{-+}^2)},$$

$$V_3=\frac{-\imath[B(k_{++}^2)-Bk_{-+}^2)]}{k_{++}^2-k_{-+}^2}, \tag{A3}$$

$$V_4=\frac{-\imath(k_{++}^2-k_{-+}^2)[A(k_{++}^2)-A(k_{-+}^2)]}{2d(k_{++},k_{-+})},$$

$$V_5=\frac{-[A(k_{++}^2)-A(k_{-+}^2)]}{2d(k_{++},k_{-+})}.$$

## APPENDIX B: INTEGRAL FOR THE ELECTRIC DIPOLE MOMENT

The integral $I_{\alpha\mu\beta}^{\mathrm{EDM}}$ becomes (after color and flavor traces)

$$I_{\alpha\mu\beta}^{\mathrm{EDM}}=\frac{2\imath N_c}{N_\rho^2}\int\frac{d^4k}{(2\pi)^4}\Gamma_\rho(k)\Gamma_\rho(k+q/2)\mathrm{tr}_D[\gamma_\beta\not{k}_{-+}\gamma_\mu\not{k}_{++}\gamma_\alpha\not{k}_{+-}T_1+\gamma_\beta\not{k}_{-+}\gamma_\mu\gamma_\alpha T_2+\gamma_\beta\not{k}_{-+}\gamma_\alpha\not{k}_{+-}k_{0+\mu}T_3$$
$$+\gamma_\beta\not{k}_{-+}\not{k}_{++}\gamma_\alpha k_{0+\mu}T_4+\gamma_\beta\not{k}_{-+}\gamma_\alpha\not{k}_{+-}k_{0+\mu}T_5+\gamma_\beta\gamma_\alpha k_{0+\mu}T_6+\gamma_\beta\not{k}_{-+}\not{k}_{++}\gamma_\alpha k_{0+\mu}T_7+\gamma_\beta\not{k}_{-+}\gamma_\alpha\not{k}_{+-}k_{0+\mu}T_8$$
$$+\gamma_\beta\not{k}_{-+}\gamma_5\sigma_{\mu\rho}q^\rho\not{k}_{++}\gamma_\alpha T_9+\gamma_\beta\not{k}_{-+}\gamma_5\sigma_{\mu\rho}q^\rho\gamma_\alpha\not{k}_{+-}T_{10}+\gamma_\beta\gamma_\mu\not{k}_{++}\gamma_\alpha T_{11}+\gamma_\beta\gamma_\mu\gamma_\alpha\not{k}_{+-}T_{12}+\gamma_\beta\gamma_\alpha k_{0+\mu}T_{13}$$
$$+\gamma_\beta\not{k}_{++}\gamma_\alpha\not{k}_{+-}k_{0+\mu}T_{14}+\gamma_\beta\not{k}_{-+}\not{k}_{++}\gamma_\alpha k_{0+\mu}T_{15}+\gamma_\beta\not{k}_{-+}\gamma_\alpha\not{k}_{+-}k_{0+\mu}T_{16}+\gamma_\beta\not{k}_{++}\gamma_\alpha\not{k}_{+-}k_{0+\mu}T_{17}+\gamma_\beta\gamma_\alpha k_{0+\mu}T_{18}$$

$$+\gamma_\beta\gamma_5\sigma\mu\rho q^\rho \not{k}_{++}\gamma_\alpha \not{k}_{+-}T_{19}+\gamma_\beta\gamma_5\sigma_{\mu\rho}q^\rho\gamma_\alpha T_{20}], \tag{B1}$$

again dropping terms with an odd number of $\gamma$ matrices. The $T_{1-20}$ are defined as follows:

$$T_1=\imath(V_1+V_4)\sigma_V(k^2_{-+})\sigma_V(k^2_{++})\sigma_V(k^2_{+-}),$$

$$T_2=-\imath(V_1+V_4)\sigma_V(k^2_{-+})\sigma_S(k^2_{++})\sigma_S(k^2_{+-}),$$

$$T_3=2\imath k^2_{++}(V_2+V_5)\sigma_V(k^2_{-+})\sigma_V(k^2_{++})\sigma_V(k^2_{+-}),$$

$$T_4=-2\imath(V_2+V_5)\sigma_V(k^2_{-+})\sigma_S(k^2_{++})\sigma_S(k^2_{+-}),$$

$$T_5=2\imath k^2_{-+}(V_2-V_5)\sigma_V(k^2_{-+})\sigma_V(k^2_{++})\sigma_V(k^2_{+-}),$$

$$T_6=-2\imath k^2_{-+}(V_2-V_5)\sigma_V(k^2_{-+})\sigma_S(k^2_{++})\sigma_S(k^2_{+-}),$$

$$T_7=-2V_3\sigma_V(k^2_{-+})\sigma_V(k^2_{++})\sigma_S(k^2_{+-}),$$

$$T_8=-2V_3\sigma_V(k^2_{-+})\sigma_S(k^2_{++})\sigma_V(k^2_{+-}),$$

$$T_9=-V_6\sigma_V(k^2_{-+})\sigma_V(k^2_{++})\sigma_S(k^2_{+-}),$$

$$T_{10}=-V_6\sigma_V(k^2_{-+})\sigma_S(k^2_{++})\sigma_V(k^2_{+-}),$$

$$T_{11}=-\imath(V_1+V_4)\sigma_S(k^2_{-+})\sigma_V(k^2_{++})\sigma_S(k^2_{+-}),$$

$$T_{12}=-\imath(V_1+V_4)\sigma_S(k^2_{-+})\sigma_S(k^2_{++})\sigma_V(k^2_{+-}),$$

$$T_{13}=-2\imath k^2_{++}(V_2+V_5)\sigma_S(k^2_{-+})\sigma_V(k^2_{++})\sigma_S(k^2_{+-}),$$

$$T_{14}=-2\imath(V_2+V_5)\sigma_S(k^2_{-+})\sigma_S(k^2_{++})\sigma_V(k^2_{+-}),$$

$$T_{15}=-2\imath(V_2-V_5)\sigma_S(k^2_{-+})\sigma_V(k^2_{++})\sigma_S(k^2_{+-}),$$

$$T_{16}=-2\imath(V_2-V_5)\sigma_S(k^2_{-+})\sigma_S(k^2_{++})\sigma_V(k^2_{+-}),$$

$$T_{17}=-2V_3\sigma_S(k^2_{-+})\sigma_V(k^2_{++})\sigma_V(k^2_{+-}),$$

$$T_{18}=2V_3\sigma_S(k^2_{-+})\sigma_S(k^2_{++})\sigma_S(k^2_{+-}),$$

$$T_{19}=-V_6\sigma_S(k^2_{-+})\sigma_V(k^2_{++})\sigma_V(k^2_{+-}),$$

$$T_{20}=V_6\sigma_S(k^2_{-+})\sigma_S(k^2_{++})\sigma_S(k^2_{+-}), \tag{B2}$$

where $V_1\cdots V_5$ are defined as before and

$$V_6=-\imath d_q, \tag{B3}$$

with $d_q$ the quark dipole moment.


[1] C. D. Roberts and A. G. Williams, Prog. Part. Nucl. Phys. **33**, 24 (1994).

[2] R. Alkofer, A. Bender, and C. D. Roberts, Int. J. Mod. Phys. A **10**, 3319 (1995).

[3] C. D. Roberts, in *Chiral Dynamics: Theory and Experiment*, Lecture Notes in Physics Vol. 452, edited by A. M. Bernstein and B. R. Holstein (Springer, Berlin, 1995), p. 68.

[4] C. D. Roberts, Nucl. Phys. **A605**, 475 (1996).

[5] M. R. Frank and C. D. Roberts, Phys. Rev. C **53**, 390 (1996).

[6] C. J. Burden, C. D. Roberts, and M. J. Thomson, Phys. Lett. B **371**, 163 (1996).

[7] K. L. Mitchell and P. C. Tandy, Phys. Rev. C **55**, 1477 (1997).

[8] R. Alkofer and C. D. Roberts, Phys. Lett. B **369**, 101 (1996).

[9] I. Chappell (private communications).

[10] M. A. Pichowsky and T.-S. H. Lee, nucl-th/9612049.

[11] P. K. Pallaghy, Ph.D. Thesis, University of Melbourne, 1996.

[12] A. Salam and R. Delbourgo, Phys. Rev. **135**, 1398 (1964).
[13] K. L. Mitchell (private communication).
[14] J. Praschifka, R. T. Cahill, and C. D. Roberts, Int. J. Mod. Phys. A **4**, 4929 (1989).
[15] P. Jain and H. Munczek, Phys. Rev. D **48**, 5403 (1993).
[16] C. J. Burden, C. D. Roberts, and A. G. Williams, Phys. Lett. B **285**, 347 (1992).
[17] Z. Dong, H. J. Munczek, and C. D. Roberts, Phys. Lett. B **333**, 536 (1994).
[18] J. S. Ball and T. W. Chiu, Phys. Rev. D **22**, 2542 (1980).
[19] D. C. Curtis and M. R. Pennington, Phys. Rev. D **42**, 4165 (1990).
[20] M. B. Hecht, University of Melbourne report, 1994.
[21] F. E. Close, *An Introduction to Quarks and Partons* (Academic, London, 1979).
[22] S. Weinberg, Phys. Rev. Lett. **37**, 657 (1976).
[23] N. Deshpande and E. Ma, Phys. Rev. D **16**, 1583 (1977).
[24] A. Chodos, R. L. Jaffe, K. Johnson, C. B. Thorn, and V. F. Weisskopf, Phys. Rev. D **9**, 3471 (1974).
[25] A. Chodos, R. L. Jaffe, K. Johnson, and C. B. Thorn, Phys. Rev. D **10**, 2599 (1974).
[26] A. W. Thomas, in *Chiral Symmetry and the Bag Model*, Advances in Nuclear Physics Vol. 13, edited by J. W. Neegle and E. Vogt (Plenum, New York, 1984), p. 1.
[27] J. Costella and B. J. H. McKellar, Report No. UM-P-92/42, 1992, (unpublished).
[28] N. E. Tupper, B. H. J. McKellar, and R. Warner, Aust. J. Phys. **41**, 19 (1988).
[29] X-G. He, B. H. J. McKellar, and S. Pakvasa, Int. J. Mod. Phys. A **4**, 5011 (1989).